

# Lipid droplets modulate proteostasis, SQST-1/SQSTM1 dynamics, and lifespan in *C. elegans*

**Anita Kumar**

Brown University

**Joslyn Mills**

Brown University

**Wesley Parker**

Brown University

**Joshua Leitão**

Brown University <https://orcid.org/0000-0002-0915-0270>

**Celeste Ng**

Brown University

**Rishi Patel**

Brown University

**Joseph Aguilera**

Brown University

**Joseph Johnson**

Brown University

**Shi Quan Wong**

Brown University

**Louis Lapierre** (✉ [louis\\_lapierre@brown.edu](mailto:louis_lapierre@brown.edu))

Brown University <https://orcid.org/0000-0002-8154-141X>

---

## Article

**Keywords:** Proteome Stability, Intestinal Lipid Stores, RNAi Screening Approach, Autophagy, Ubiquitination of Proteins, Alzheimer's Disease

**Posted Date:** May 7th, 2021

**DOI:** <https://doi.org/10.21203/rs.3.rs-452997/v1>

**License:** © ⓘ This work is licensed under a Creative Commons Attribution 4.0 International License.

[Read Full License](#)

---

1 **Lipid droplets modulate proteostasis, SQST-1/SQSTM1 dynamics, and lifespan in *C.***  
2 ***elegans***

3 Anita V. Kumar<sup>#</sup>, Joslyn Mills<sup>#</sup>, Wesley M. Parker<sup>#</sup>, Joshua A. Leitão<sup>#</sup>, Celeste Ng, Rishi Patel,  
4 Joseph L. Aguilera, Joseph R. Johnson, Shi Quan Wong and Louis R. Lapierre<sup>\*</sup>

5 *Department of Molecular Biology, Cell Biology and Biochemistry, Brown University, 185 Meeting*  
6 *St., Providence, Rhode Island 02912, USA*

7 <sup>#</sup>: Equal contributions

8 <sup>\*</sup>: Correspondence addressed to L.R.L. (louis\_lapierre@brown.edu)

9

10 **ABSTRACT**

11 The ability of organisms to live long depends largely on the maintenance of proteome stability via  
12 proteostatic mechanisms including translational regulation, protein chaperoning and degradation  
13 machineries. In several long-lived *Caenorhabditis elegans* strains, such as insulin/IGF-1 receptor  
14 *daf-2* mutants, enhanced proteostatic mechanisms are accompanied by elevated intestinal lipid  
15 stores, but the role of lipid droplets in longevity has remained obscure. Here, while determining  
16 the regulatory network of the selective autophagy receptor SQST-1/SQSTM1, we unexpectedly  
17 uncovered a novel role for lipid droplets in proteostasis and longevity. Using an unbiased genome-  
18 wide RNAi screening approach, we identified several SQST-1 modulators, including proteins  
19 found on lipid droplets and those prone to aggregate with age. SQST-1 accumulated on lipid  
20 droplets when autophagy was inhibited, suggesting that lipid droplets may serve a role in  
21 facilitating selective autophagy. Expansion of intestinal lipid droplets by silencing the conserved  
22 cytosolic triacylglycerol lipase gene *atgl-1/ATGL* enhanced autophagy, and extended lifespan in  
23 an HSF-1/HSF1-dependent and CDC-48/VCP-dependent manner. Silencing *atgl-1* mitigated the  
24 age-related accumulation of SQST-1 and reduced overall ubiquitination of proteins. Reducing  
25 *atgl-1* also improved proteostasis in a nematode model of Alzheimer's disease. Subcellular  
26 analyses revealed that lipid droplets unexpectedly harbor more ubiquitinated proteins than the

27 cytosol. Accordingly, low lipid droplet levels exacerbated the proteostatic collapse when  
28 autophagy or proteasome function was compromised. Altogether, our study uncovers a key role  
29 for lipid droplets in *C. elegans* as a proteostatic mediator that reduces protein ubiquitination,  
30 facilitates autophagy, and promotes longevity.

31

## 32 INTRODUCTION

33 One of the major hallmarks of aging is the accumulation of damaged proteins that progressively  
34 compartmentalize in inclusions and aggregates<sup>1</sup>. In the nematode *C. elegans*, several proteins  
35 display impaired solubility with age<sup>2,3</sup>. This phenomenon suggests that mechanisms that mediate  
36 protein stabilization, such as chaperone-mediated folding and post translational modifications,  
37 actively contribute to somatic maintenance by preventing the collapse of the proteome<sup>4,5</sup>. The  
38 enhanced proteasomal<sup>6</sup> and autophagic<sup>7,8</sup> capacities, the increased chaperone function<sup>9</sup> and  
39 alterations in ribosomal biogenesis<sup>10</sup> and function<sup>11,12</sup> in long-lived nematodes support the notion  
40 that the balance between synthesis, folding, and efficient clearance of proteins is important for  
41 conferring organismal longevity.

42 Generally, proteins destined for degradation are tagged via poly-ubiquitination and recognized by  
43 ubiquitin binding domain-containing proteins that direct cargo toward proteasomal or autophagic  
44 degradation. The autophagy receptor, Sequestosome 1 (SQST-1/SQSTM1) is a well-established  
45 and conserved mediator of cargo recognition, which includes ubiquitinated targets<sup>13</sup>. The SQST-  
46 1-cargo complex can interact with the autophagosome proteins LGG-1/GABARAP and LGG-  
47 2/LC3 to enable cargo sequestration in the nascent autophagosome<sup>14</sup>. Notably, SQST-  
48 1/SQSTM1 has emerged as a potential lifespan modulator in nematodes and flies<sup>15-17</sup>.  
49 Additionally, selective autophagy of mitochondria has been linked to longevity<sup>18</sup>, suggesting that  
50 autophagic degradation of specific cargos and organelles is beneficial against organismal aging.  
51 Although SQST-1/SQSTM1 has been implicated in the selective clearance of aggregated

52 proteins<sup>19</sup>, much remains to be understood about the modulation of this autophagy receptor, its  
53 cargoes, and the nature and extent of its contribution to lifespan.  
54 In nematodes, intestinal cells have a unique role in autophagy-mediated longevity as they manage  
55 nutrient influx and signals from neurons<sup>20</sup> and the germline<sup>21</sup> to coordinate appropriate responses  
56 necessary for organismal survival. In particular, intestinal autophagy genes are required for  
57 lifespan extension<sup>22</sup> by maintaining intestinal tissue integrity and proteostasis. Intestinal cells are  
58 also sites of dynamic lysosomal function<sup>23-26</sup> that mediate specific longevity-associated lipid  
59 signaling<sup>27-29</sup>. Intriguingly, several established long-lived animals including *daf-2*, *glp-1* and *rsks-*  
60 *1* mutants also maintain unusually large intestinal lipid droplet stores throughout their life<sup>30-33</sup>.  
61 Accordingly, redistributing lipids intended for secreted lipoproteins to intestinal lipid droplets is  
62 sufficient to extend lifespan<sup>29</sup>. However, in long-lived animals, it is unclear whether adult intestinal  
63 lipid stores are simply a consequence of reduced demand from the germline<sup>34</sup>, a long-term energy  
64 store rationing strategy<sup>35</sup> or a more direct mediator of somatic maintenance. Here, while  
65 identifying the regulatory network of SQST-1, we found that lipid droplet accumulation in long-  
66 lived nematodes represents a novel proteostatic mechanism that reduces overall SQST-1 and  
67 ubiquitination levels, and mitigates age-related proteostatic stress.

68

## 69 **RESULTS**

### 70 *SQST-1 accumulation is detrimental to lifespan in C. elegans*

71 We initially considered the possibility that increasing SQST-1 may improve proteostasis by  
72 enhancing the ability of cells to mediate selective autophagy. We hypothesized that increasing  
73 the expression of a receptor that recognizes ubiquitinated cargoes may suffice in driving their  
74 degradation. While this study was being conducted, the Hansen laboratory showed that over-  
75 expressing SQST-1 can extend lifespan at 20°C<sup>16</sup>. Since longevity interventions and temperature  
76 mechanistically interact<sup>36</sup>, we examined lifespan at both 20°C and 25°C using several over-

77 expressing strains (*psqst-1::sqst-1::rfp*, *psqst-1::sqst-1::gfp::rfp*), including two created in the  
78 Hansen laboratory (*psqst-1::sqst-1::gfp* and *psqst-1::sqst-1*)<sup>16</sup>. Over-expression of SQST-1 was  
79 unexpectedly detrimental at 25°C (**Figure 1a-c**, **Supplemental Figure 1a-c**) and was not  
80 sufficient to extend lifespan at 20°C (**Figure 1d-f**). While contradictory to recent literature<sup>16</sup>, these  
81 findings are in line with most studies about the autophagy pathway and aging, i.e. that over-  
82 expressing an autophagy receptor might not necessarily be sufficient to improve lifespan<sup>37</sup>. A  
83 closer investigation into the temperature-dependent differences in lifespan revealed marked  
84 upregulation of *sqst-1* mRNA at higher temperature in these strains (from ~5-fold in wild-type, up  
85 to ~75 fold in SQST-1::GFP over-expressing animals) (**Figure 1g**). In order to measure the active  
86 trafficking of SQST-1 into the lysosome as a guide for selective autophagy, we developed a  
87 tandem reporter system expressing SQST-1 fused to both GFP and RFP<sup>7</sup> (GFP signal is  
88 quenched in low pH environments). We confirmed that the conversion of tandem SQST-1 into an  
89 RFP-only signal is reduced in autophagy-deficient *atg-18* mutants (**Supplemental Figure 1d**).  
90 While relatively modest at 20°C (**Figure 1h-i**), increasing temperature up to 30°C for 24 hours  
91 significantly enhanced the conversion to the RFP-only tandem SQST-1 signal, suggesting that  
92 selective autophagy is induced with heat stress. Over-expressing SQST-1 at 25°C was also  
93 accompanied by higher levels of total ubiquitinated proteins and we found substantial  
94 temperature-dependent intestinal and neuronal accumulation of SQST-1 during aging (**Figure 1a-**  
95 **f inset and Supplemental Figure 1e-h**). While over-expressing SQST-1 was detrimental at 25°C,  
96 so was the loss of *sqst-1* (**Supplemental Figure 1i-j**), suggesting that SQST-1 function has a  
97 temperature-specific role in the lifespan of wild-type animals. Expression and steady-state levels  
98 of SQST-1 likely need to be tightly coordinated with cargo targeting and more importantly, with  
99 the rate of protein degradation systems (i.e. autophagy and proteasome). Altogether, we found  
100 that solely increasing SQST-1 is detrimental for lifespan at 25°C and inconsequential at 20°C,  
101 indicating a temperature-dependent effect on SQST-1 dynamics in aging.

102 *Proteins that bind lipid droplets modulate SQST-1 dynamics*

103 In order to better understand how SQST-1 is regulated, we opted for an unbiased genome-wide  
104 RNAi screening approach in an integrated SQST-1 over-expressing strain (*psqst-1::sqst-1::gfp*)  
105 at 25°C during development. SQST-1 modulators were subsequently validated by gene silencing  
106 in a separate over-expressing strain (*psqst-1::sqst-1::rfp*) during development and adulthood.  
107 Interestingly, the vast majority of modifiers led to the intestinal accumulation of fluorescently  
108 tagged SQST-1 in both development and adulthood (**Supplemental Table 1**). A substantial  
109 portion of genetic modifiers clustered in ribosomal-related proteins, including proteins coding for  
110 small and large subunits, suggesting that ribosomal assembly and function substantially impact  
111 SQST-1 dynamics (**Figure 2a, Supplemental Table 1**). This is in line with studies in *C. elegans*<sup>2</sup>  
112 and killifish<sup>38</sup>, highlighting the age-related instability of several ribosomal proteins and consequent  
113 ribosomal mis-assembly. Since autophagy inhibition by silencing *lgg-1* led to substantial  
114 accumulation of droplet-like structures in the intestine (**Figure 2b**), we wondered if SQST-1 might  
115 associate with lipid droplets. We co-expressed SQST-1::RFP and the lipid resident protein DHS-  
116 3 fused to GFP<sup>39</sup> in nematodes and we found that close to 50% of SQST-1::RFP localizes to lipid  
117 droplets when autophagy is inhibited (**Figure 2c**). Thus, we investigated whether SQST-1  
118 modulators may also be related to lipid droplet metabolism. We compared our SQST-1  
119 modulators to proteins that have been found to bind lipids<sup>40</sup> and found significant overlap ( $p <$   
120  $8.253e-65$ ) (**Figure 2d**). Interestingly, several proteins prone to age-dependent aggregation<sup>2</sup> also  
121 modulated SQST-1 accumulation ( $p < 2.923e-11$ ) (**Figure 2d**). Overall, 19 SQST-1 modulators  
122 have the propensity to both aggregate with age and bind lipid droplets (**Figure 2e-f,**  
123 **Supplemental Table 2**). Several ribosomal subunits (*rps* and *rpl* genes) and mRNA-related  
124 proteins (*inf-1* and *pab-1*) emerged, along with the HSP70 chaperone family member *hsp-*  
125 *1/HSPA8*, indicating that ribosomal assembly, translation initiation, and protein folding are  
126 important regulators of SQST-1 dynamics (**Figure 2e-f**). Here, our comparative analysis suggests

127 that progressive SQST-1 accumulation may be partly attributed to altered interactions between  
128 lipid droplets and intrinsically unstable proteins.

129 *Elevated lipid droplets reduce SQST-1 accumulation and extend lifespan*

130 Intestinal lipid droplet accumulation is a striking feature of several long-lived nematodes<sup>30-32</sup>. Since  
131 SQST-1 accumulated on lipid droplets when autophagy was inhibited (**Figure 2c**), and several  
132 SQST-1 modifiers bind lipid droplets (**Figure 2d**), we speculated that lipid droplets may underlie  
133 the ability of long-lived animals to stabilize or facilitate clearance of potentially aggregating  
134 proteins and maintain proteome stability during aging. In order to specifically stimulate intestinal  
135 lipid droplet accumulation and expansion, we silenced the conserved cytosolic lipase *atgl-1/ATGL*  
136<sup>41</sup> during adulthood to attenuate lipid droplet breakdown, which led to larger lipid stores thereby  
137 mimicking a key feature of several long-lived animals (**Figure 3a, inset**). Silencing *atgl-1* resulted  
138 in a significant lifespan extension in wild-type animals (12-28%), indicating that lipid droplet  
139 accumulation is sufficient to mediate longevity (**Figure 3a-b**). This observation pointed to a  
140 possible lipid droplet-mediated cytoprotective mechanism<sup>42</sup>. Indeed, silencing *atgl-1* in SQST-  
141 1::RFP over-expressing animals led to a substantial increase in lifespan (**Figure 3c**) accompanied  
142 by a marked decrease in SQST-1 accumulation (**Figure 3d**). Similar observations were made in  
143 animals over-expressing SQST-1::GFP (**Supplemental Figure 2a**), suggesting that the lipid  
144 droplet-mediated effects precede SQST-1-mediated selective autophagy.

145 To determine whether accumulation of lipids is able to improve the lifespan of proteostatically-  
146 impaired mutants, we silenced *atgl-1* in three well-established short-lived mutants, including *daf-*  
147 *16(mu86)*, *hlh-30(tm1978)*, and *hsf-1(sy441)*<sup>43</sup>. Notably, the expression of these transcription  
148 factors was increased at 25°C compared to 20°C, suggesting that their function may be stimulated  
149 by heat (**Supplemental Figure 2b**). Silencing *atgl-1* extended the lifespan of *daf-16* and *hlh-30*  
150 mutants, but not the lifespan of *hsf-1* mutants (**Figure 3e-g**), indicating that lipid droplet-mediated  
151 lifespan extension may require the expression of key chaperones regulated by HSF-1/HSF1, such  
152 as heat shock protein HSP-1, which binds lipid droplets and modulates SQST-1 levels (**Figure**

153 **2e-f**). Interestingly, lipid droplets may harbor chaperones with roles in aggregate clearance<sup>44</sup>.  
154 Notably, autophagic activity, as measured by the tandem mCherry::GFP::LGG-1 reporter<sup>7</sup>,  
155 showed that *atgl-1* silencing increases the conversion of autophagosomes into autolysosomes  
156 (**Figure 3h, Supplemental Figure 2c**). Altogether, our data favors a model by which lipid droplets  
157 work in concert with HSF-1-regulated chaperones to enhance proteostasis, autophagy, and  
158 lifespan.

159 As our lifespan analyses highlighted novel proteostatic and longevity roles for lipid droplets, we  
160 reasoned that long-lived animals with large lipid stores should accumulate less intestinal SQST-  
161 1. Strikingly, *daf-2(e1370)* expressing SQST-1::GFP (**Figure 3i**) or SQST-1::RFP (**Supplemental**  
162 **Figure 2d**) accumulated negligible intestinal SQST-1 during aging (GFP signal in mid-section was  
163 entirely gonadal, see wild-type comparison in **Figure 1b**). In addition, SQST-1 over-expression  
164 did not significantly affect the long lifespan of *daf-2* animals (**Figure 3i**). Loss of *sqst-1* did not  
165 affect the lifespan of *daf-2* animals (**Supplemental Figure 2e**), as previously shown<sup>16</sup>, highlighting  
166 that SQST-1 function becomes less important at 25°C for the lifespan of organisms with relatively  
167 stable proteomes. The extent of heat-induced increase in SQST-1-mediated selective autophagy  
168 was also attenuated in *daf-2* animals (**Supplemental Figure 2f**), suggesting that elevated lipid  
169 droplets may buffer the need for SQST-1 function during heat stress. Silencing *atgl-1* in *daf-2*  
170 animals enhanced their intestinal lipid stores and further extended their lifespan (**Figure 3j**),  
171 indicating that elevated lipid droplet accumulation can also extend lifespan in animals with  
172 enhanced proteostasis. Altogether, our data present an important and previously unrecognized  
173 role for lipid droplets in SQST-1 dynamics and longevity.

174

#### 175 *Silencing atgl-1 elicits limited changes in gene expression*

176 Lipid droplets have been recently shown to coordinate transcriptional programs by sequestering  
177 factors that modulate transcription<sup>45</sup>. Since HSF-1 was required for lifespan extension by *atgl-1*  
178 silencing, we hypothesized that the lipid droplet increase associated with *atgl-1* silencing might



179 affect the expression of HSF-1-regulated targets. Using RNA sequencing (RNA-seq), we found  
180 that enhancing lipid stores by silencing *atgl-1* in WT or *daf-2* animals had limited effect on global  
181 transcription. Silencing *atgl-1* resulted in 13 overlapping differentially expressed genes (DEG) in  
182 wild-type animals and *daf-2* mutants of which 7 genes are down-regulated in both cases  
183 (**Supplemental Figure 3a-b**). Altering *atgl-1* levels (silencing or over-expression) led to  
184 differential expression of 50 overlapping genes, with no discernable transcription factor signature  
185 (**Supplemental Figure 3c-d**). In addition, expression of *sqst-1* was unchanged in wild-type  
186 animals with low or high levels of *atgl-1*. Overall, we concluded that transcriptional regulation may  
187 not contribute significantly to the proteostatic-enhancing and lifespan-extending effects of lipid  
188 droplets. Therefore, lipid droplets may impact proteostasis via a more direct mechanism on the  
189 proteome itself.

190

#### 191 *Lipid droplets enhance proteostasis by modulating the accumulation of ubiquitinated proteins*

192 The emerging connection between lipid droplet stores and proteome stability led us to investigate  
193 how lipid droplet loss affects proteostasis and SQST-1 abundance. First, we tested whether lipid  
194 droplet depletion affects lifespan using ATGL-1::GFP over-expressing animals<sup>46</sup>. Unlike at 20°C  
195 (**Supplemental Table 3**)<sup>47</sup>, we found that over-expressing ATGL-1 was detrimental to lifespan at  
196 25°C (**Figure 4a**) and led to a significant increase in SQST-1 intestinal accumulation  
197 accompanied by lower lipid stores (**Figure 4b**), suggesting that loss of lipid droplet stores can  
198 interfere with SQST-1 dynamics. When autophagy or proteasome function was reduced by  
199 silencing autophagosome protein *lgg-1* or proteasome subunit *rpn-6.1*, respectively, ubiquitinated  
200 protein levels were higher in animals with lower lipid stores, suggesting that lipid droplets may  
201 buffer the proteome and facilitate the processing of unstable or misfolded proteins (**Figure 4c**).  
202 Strikingly, analyzing lipid droplets in wild-type animals revealed preferential accumulation of  
203 ubiquitinated proteins in lipid droplet-enriched fractions (**Figure 4d**), indicating that lipid droplets

204 contain a significant amount of proteins bound for degradation. Lipid droplet-associated  
205 accumulation of ubiquitinated proteins was increased when autophagic or proteasomal  
206 degradation was reduced (**Figure 4d**), suggesting that lipid droplets have the capacity to harbor  
207 many degradation cargoes, which may become particularly relevant for proteostasis when  
208 autophagic and proteasomal systems are failing during aging.

209 The association and function of ATGL-1 with lipid droplets was recently found to be antagonized  
210 by the AAA-ATPase CDC-48/VCP<sup>48</sup>. CDC-48/VCP is best known for its role in ER-associated  
211 degradation machinery<sup>49</sup>, but it has been associated with other functions including endocytosis<sup>50</sup>  
212 and more recently autophagy itself<sup>51</sup>. CDC-48/VCP helps unfold unstable, ubiquitinated, and  
213 proteasomal degradation-bound proteins in concert with heat shock protein HSP-70, a key  
214 regulated target of HSF-1<sup>52</sup>. Thus, we assayed the effect of the loss of CDC-48 on SQST-1 and  
215 ATGL-1 levels using fluorescent reporters. Silencing *cdc-48.2* increased the levels of ATGL-  
216 1::GFP (**Supplemental Figure 4a**) and led to the accumulation of SQST-1::RFP (**Supplemental**  
217 **Figure 4b**). In mammalian cells, loss of proteasome function drives SQSTM1 to divert cargo to  
218 selective autophagy<sup>53</sup>, but stimulating proteasomal processing by over-expressing of VCP can  
219 reduce SQSTM1 accumulation<sup>54</sup>. Here, we reasoned that CDC-48 functions related to processing  
220 ubiquitinated targets and autophagy may underlie the ability of nematodes with elevated lipid  
221 droplets to attenuate SQST-1 accumulation and modulate lifespan. Accordingly, silencing *atgl-1*  
222 in *cdc-48.1* or *cdc-48.2* mutants failed to significantly extend lifespan (**Supplemental Figure 4c**,  
223 **Supplemental Table 4**), indicating that lipid droplet-mediated lifespan extension requires  
224 functional CDC-48.

225 As lipid droplet size increases, its surface also increases, and it is possible that the capacity of  
226 this organelle to bind and stabilize proteins may also increase as well. Enhancing lipid droplet  
227 stores by silencing *atgl-1* reduced the overall accumulation of ubiquitinated proteins, in particular  
228 in the lower solubility (5% SDS soluble) fraction (**Figure 4e**), suggesting that typically insoluble  
229 proteins are less likely to be ubiquitinated when lipid droplets abound. Notably, the types of

230 proteins that aggregate with age differ between wild-type and long-lived *daf-2* mutants, as the  
231 latter tends to accumulate aggregating proteins that are less hydrophobic than those aggregating  
232 in wild-type animals<sup>4</sup>. Reducing lipid droplet stores genetically by silencing lipogenic genes *sbp-*  
233 *1(SREBP2)*, *lpin-1(LIPN1)* or *fasn-1(FASN)* enhanced SQST-1 accumulation in wild-type animals  
234 (**Supplemental Figure 4d**). Similarly, loss of lipid droplet stores by silencing *lpin-1* in *daf-2*  
235 resulted in increased SQST-1 accumulation and overall protein ubiquitination (**Figure 4f-g**). As  
236 proteostasis failure is a feature of neurodegeneration, we tested the effect of increasing lipid  
237 droplet levels in a proteotoxic context. Reducing the expression of *atgl-1* in a proteotoxic model  
238 of Alzheimer's disease resulted in a marked protection against aggregation-associated paralysis<sup>55</sup>  
239 (**Figure 4h**). Altogether, our data demonstrate that lipid droplets are important for proteostasis  
240 and contribute to lifespan by facilitating autophagy and stabilizing the proteome.

241

## 242 **DISCUSSION**

243 Decades of aging research has uncovered key longevity-regulating pathways in *C. elegans*<sup>43</sup>, yet  
244 the role of lipid droplets in the lifespan of several established long-lived nematodes has remained  
245 unresolved. Here, while studying the regulation of the selective autophagy receptor SQST-1, we  
246 unexpectedly uncovered a direct role for lipid droplets in proteostasis and lifespan. Several SQST-  
247 1 modulators associate with lipid droplets and aggregate with age, including ribosomal,  
248 translation-related, and folding-related proteins<sup>40</sup>, supporting the mechanism that ribosomal  
249 assembly dysfunction due to loss in subunit stoichiometry may burden the autophagy machinery,  
250 and contribute to age-related proteotoxicity<sup>38</sup>. Importantly, lipid droplet accumulation, by silencing  
251 cytosolic triacylglycerol lipase *atgl-1/ATGL*, mitigates the progressive age-related SQST-1  
252 accumulation, a benefit recapitulated in long-lived, lipid droplet-rich *daf-2* mutant animals. Lipid  
253 droplets are cytoprotective as they prevent aberrant SQST-1 accumulation, in part via the  
254 functioning of AAA-ATPase CDC-48/VCP which processes ubiquitinated proteins for proteasomal  
255 degradation<sup>56</sup>. Strikingly, we found that the majority of ubiquitinated proteins in nematodes was

256 associated with lipid droplets, suggesting that unstable proteins bound for degradation may be  
257 stabilized by the surface of lipid droplets. Our findings also provide support to the importance of  
258 the emerging lipid-droplet-mediated protein degradation process<sup>57,58</sup> in longevity and aging.  
259 Altogether, our study strengthens the emerging concept that lipid droplets serve as a buffer for  
260 proteostasis<sup>42</sup> by stabilizing proteomes and coordinating protein degradation machineries.  
261 Understanding the regulation of SQST-1/SQSTM1 during aging and in different disease contexts  
262 is important in order to determine the validity of stimulating selective autophagy as a therapeutic  
263 strategy to improve proteostasis in age-related diseases<sup>59</sup>. Here, we find that over-expressing  
264 SQST-1 had no effect on the lifespan of wild-type animals at 20°C<sup>16</sup> whereas elevated SQST-1  
265 level at 25°C was detrimental. In hindsight, one may have predicted that over-expressing a  
266 ubiquitin-binding protein with a propensity for oligomerization<sup>60</sup> might not be necessarily  
267 advantageous, particularly in organisms nearing their protein solubility limit<sup>2,3</sup> and displaying  
268 overall proteome instability during aging<sup>5</sup>. SQST-1 over-expression was primarily visible in  
269 neuronal and intestinal cells and accumulates in a temperature-dependent manner and  
270 progressively during aging. The inability of stressed and aging animals to process ubiquitinated  
271 cargos bound for proteasomal or autophagic degradation may lead to a gradual build-up of SQST-  
272 1. Accordingly, SQST-1 over-expression may over-sensitize the animals to unstable,  
273 ubiquitination-prone proteins, posing an additional challenge to the autophagic machinery. This  
274 is exemplified by recent evidence that reducing SQST-1 specifically in the neurons of a nematode  
275 model of ALS is protective<sup>61</sup>, possibly since mutant fused in sarcoma (FUS) expression promotes  
276 SQST-1 accumulation, which exacerbates proteotoxicity and neurodegeneration. Notably,  
277 SQSTM1 can phase separate when interacting with ubiquitinated cargoes<sup>62</sup>, but the impact of the  
278 formation of these condensates on overall proteostasis is unclear.  
279 Lipid droplet accumulation is a prominent and under-explored phenotype of several long-lived  
280 nematodes, including well-established models such as germline-less *glp-1* animals, protein

281 translation *rsks-1* mutants, insulin/IGF-1 receptor *daf-2* mutants<sup>63</sup> as well as in long-lived animals  
282 with reduced nuclear export<sup>64</sup>. In addition, lifespan extension by inhibiting intestinal lipid secretion  
283 mediated by vitellogenins results in lipid redistribution to intestinal lipid droplet stores<sup>29</sup>, a process  
284 believed to generate precursors for lysosomally-derived lipid signals<sup>28</sup>. While enhanced lysosomal  
285 lipolysis and lipophagy may stimulate longevity-associated lipid signaling, overactive cytosolic  
286 lipolysis decreases the ability of cells to maintain a stable proteome, which may burden the  
287 selective autophagy machinery. Our findings support that lipid droplets are much more than just  
288 lipid storage organelles<sup>42</sup> and can serve as interfaces to enable protein stabilization and  
289 processing.

290 Rationing of intestinal lipid stores was originally evoked as a potential mechanism to provide long-  
291 term energy for dauer larvae that arrest feeding<sup>35</sup>. Here, we propose a role for lipid stores during  
292 adulthood that focuses on their capacity to buffer proteostasis during aging in concert with heat  
293 shock chaperones, thereby unburdening protein degradation systems (**Figure 5**). ATGL-1 over-  
294 expression leads to lipid store depletion, but, more importantly, it also removes the protection  
295 conferred by lipid droplets and renders animals vulnerable to proteotoxic stress associated with  
296 reduced proteasomal function, heat and aging. Our data also show that the lipid droplet-mediated  
297 decrease in protein ubiquitination and the enhancement in lifespan require the function of the  
298 AAA-ATPase CDC-48/VCP, a ubiquitin protein processing enzyme and autophagy modulator<sup>51</sup>.

299 Lipid droplet expansion may belong to an arsenal of proteostatic measures that lipid-storing cells  
300 and possibly neurons can employ to prevent protein misfolding and aggregation. While lipid  
301 droplet accumulation in immune cells such as macrophages<sup>65</sup> and microglia<sup>66</sup> may be  
302 inflammatory and contribute to aging, lipid droplets may confer some post-mitotic, differentiated  
303 cells with added protection against protein aggregation<sup>44</sup> and mitochondrial lipid overload<sup>67</sup>. For  
304 example, lipid droplet accumulation in Alzheimer's disease pathogenesis<sup>68</sup> may highlight an effort  
305 from neuronal cells to improve proteome stability and resilience against progressive  
306 proteotoxicity. Notably, drastic inhibition of triacylglycerol lipolysis becomes detrimental to

307 neurons<sup>69</sup> as larger lipid droplets are less easily broken down<sup>46</sup>. However, a recent study showed  
308 that lipid droplet accumulation protected hyper-activated neurons from cell death<sup>70</sup>, a  
309 phenomenon potentially relevant in Alzheimer's disease<sup>71</sup>. Thus, moderate accumulation of lipid  
310 droplets may be more desirable to provide protection against age-related proteotoxicity. In  
311 agreement, our data show marked protection against paralysis in a proteostatic Alzheimer's  
312 disease model by attenuating cytosolic lipolysis.

313 Enhancing proteostasis by stimulating the autophagy process has emerged as an attractive  
314 strategy to mitigate several age-related diseases with pathological proteostatic decline such as  
315 neurodegenerative diseases<sup>72</sup>. However, our study indicates that stimulating selective autophagy  
316 by specifically increasing the expression of one selective autophagy receptor, SQST-1/SQSTM1,  
317 is not sufficient to improve proteostasis and may exacerbate age-related proteostatic collapse.  
318 Overall, our study suggests that therapeutic improvement in proteostasis may benefit from a  
319 combinatorial approach in which the whole autophagy/lysosomal machinery is stimulated  
320 concomitantly with a modest reduction in lipid droplet breakdown. Such an approach may prevent  
321 pathogenic burdening of the autophagy/lysosome pathway with cargoes that could have  
322 otherwise been stabilized by lipid droplets or routed to the proteasome.

323

## 324 **METHODS**

### 325 ***C. elegans* strain maintenance**

326 Nematodes were maintained at 20°C on agar NGM plates seeded with OP50 *E. coli* unless  
327 otherwise noted, as previously described<sup>73</sup>. Synchronized populations were prepared using a  
328 sodium hypochlorite solution to collect eggs as previously described<sup>74</sup>. Supplemental Tables 5  
329 and 6 contains the list of strains used in this study. HT115 *E. coli* and RNAi clones from the  
330 Ahringer library (Source Bioscience) were used for RNAi experiments<sup>75</sup>.

331

### 332 **Transgenic strain construction**

333 DNA constructs for the plasmids pLAP26 (*psqst-1::sqst-1::rfp::unc-54 3'UTR*) and pLAP29 (*psqst-*  
334 *1::sqst-1::gfp::rfp::unc-54 3'UTR*) were assembled using HiFi cloning and were injected into the  
335 germline of Day 1 adults (pLAP26 was co-injected with the pLAP7 (*myo-2::gfp::unc-54*)).  
336 Transgenic progeny was UV-irradiated for extrachromosomal array integration and selected for  
337 100% transmission rate and backcrossed at least four times to wildtype N2. Details about strain  
338 construction are provided in Supplemental Table 6.

339

### 340 **Genome-wide RNAi screen**

341 Approximately 50 synchronized transgenic eggs (*psqst-1::SQST-1::GFP*) were transferred onto  
342 plates seeded with RNAi against all genes from the Ahringer library (Source BioScience), which  
343 represents about 86% of the predicted genes in the *C. elegans* genome<sup>75</sup>. Nematodes were  
344 developed at 25°C and changes in GFP intensity or expression pattern were monitored on Day 1  
345 of adulthood. As a negative control, bacteria expressing the L4440 backbone (i.e. empty vector)  
346 expressed in HT115 *E. coli* were used. Hits from the genome-wide RNAi screen were sequenced  
347 (GENEWIZ), validated three times and corroborated using transgenic animals expressing *SQST-*  
348 *1::RFP*. RNAi against the genes with the strongest effect on GFP expression were subsequently  
349 validated by silencing in adulthood only. Details are provided in Supplemental Tables 1 and 2.

350

### 351 **Lifespan analyses**

352 Eggs obtained from bleaching were transferred onto OP50 *E. coli* bacteria-seeded agar plates.  
353 All lifespan analyses were carried out at 25°C starting at Day 1 of adulthood after development at  
354 20°C, unless otherwise noted. For gene knockdown experiments, worms were transferred to  
355 bacteria expressing corresponding RNAi at day one of adulthood. Viability was scored every 1 to  
356 3 days, as previously described<sup>76</sup>. Survival curves and statistical analysis were generated using  
357 the Stata 15.0 software (StataCorp). Details are provided in Supplemental Tables 3 and 4.

358

359 **Comparative analyses**

360 Knocked-down genes with the strongest effect on SQST-1::GFP levels were analyzed for gene  
361 ontology using WormCat<sup>77</sup> to identify which pathways were enriched. RNAi against genes that  
362 overlapped with the SQST-1 modulators, lipid droplet proteome<sup>40</sup>, and insoluble proteins<sup>2</sup> were  
363 then tested in adult-only experiments. Statistical significance of the overlap between any two  
364 groups of genes was calculated by hypergeometric probability (nemates.org, Lund laboratory,  
365 University of Kentucky). For adult-only RNAi validation, eggs from wild-type and SQST-1  
366 transgenic animals were developed on OP50 *E coli*. bacteria at 20°C and transferred to  
367 corresponding RNAi plates at Day 1 of adulthood and grown at 25°C for an additional 72 hours.  
368 Adults were transferred away from their progeny and bright field and fluorescent images were  
369 taken daily.

370

371 **Imaging and analyses**

372 Worms were visualized using a Zeiss Discovery V20 fluorescence dissecting microscope (Zeiss,  
373 White Plains, NY). Worms were immobilized with 0.1% sodium azide in M9 solution (42 mM  
374 Na<sub>2</sub>HPO<sub>4</sub> 22 mM KH<sub>2</sub>PO<sub>4</sub> 86 mM NaCl, 1 mM MgSO<sub>4</sub>·7H<sub>2</sub>O) on agar plates and images were  
375 taken via Zen imaging software, using consistent parameters (magnification and exposure)  
376 within each experiment. For quantification of fluorescent signal, total fluorescence of each worm  
377 in each image was analyzed using ImageJ software and averaged for mean total fluorescence.  
378 Confocal microscopy images were obtained on an Olympus FV3000 inverted confocal laser  
379 scanning microscope (Leduc Bioimaging Facility, Brown University). Quantification of  
380 autophagosomes and autolysosomes in the LGG-1 tandem reporter strain and overlap between  
381 lipid droplet protein (DHS-3) and tagged SQST-1 in the over-expressing strain was performed  
382 using color thresholding and particle analysis functions in ImageJ (NIH).

383

384 **Lipid staining**



385 Worms were collected and washed twice with M9 solution and then fixed with 60% isopropanol  
386 for 30 minutes. After fixation, worms were stained overnight on a rocker with freshly prepared  
387 60% Oil Red O (stock solution of 0.5% ORO in isopropanol diluted with water, equilibrated  
388 overnight on a rocker, and gravity-filtered). The following day, worms were washed with TBS-T  
389 (50 mM Tris base, 150 mM Tris HCl, 1.5 M NaCl, and 0.05% Tween-20) and imaged using a  
390 Zeiss Discovery V20 fluorescence dissecting microscope.

391

### 392 **Gene expression analysis**

393 RNA was extracted from approximately 3,000 Day 1 worms and cDNA was prepared as  
394 previously described<sup>8</sup>. Gene expression levels were measured in biological triplicates using iTaq  
395 Universal SYBR Green Supermix (BIO-RAD), and a Roche LightCycler 96 (Indianapolis, IN).  
396 Expression was normalized using 2 housekeeping genes, *act-1* and *cyn-1* and statistical analyses  
397 were performed using GraphPad Prism 7 (GraphPad Software). See Supplemental Table 7 for  
398 qPCR primers details.

399

### 400 **RNAseq sample preparation and analysis**

401 WT or *daf-2* mutant worms were developed on OP50 at 20°C and transferred to corresponding  
402 RNAi plates at Day 1 of adulthood and grown at 25°C for an additional 96 hours. Worms over-  
403 expressing ATGL-1::GFP were developed on OP50 at 20°C and grown at 25°C for an additional  
404 96 hours. Adults were transferred away from their progeny daily. RNA was extracted and cDNA  
405 was prepared as previously described<sup>8</sup>. RNA quality was confirmed by BioAnalyzer (Genomics  
406 Core, Brown University), and *atgl-1* silencing was confirmed by qPCR before submitting samples  
407 for RNAseq analysis by GENEWIZ as previously described<sup>8</sup>.

408

### 409 **Lipid droplet fractionation**

410 Lipid droplets were isolated by ultracentrifugation from 24,000 Day 5 animals grown at 25°C on  
411 RNAi for 96 hours. Worms were homogenized with a ball-bearing homogenizer in MSB buffer  
412 (250mM sucrose and 10mM Tris-HCl pH 7.4) containing protease inhibitor (Roche). The lysate  
413 was cleared of cuticle debris and unlysed worms by centrifuging at 500 x g for 5 minutes. 10% of  
414 the cleared lysate was reserved as “Input”. Nuclei and non-lipid droplet organelles were pelleted  
415 out of the cytosol by an ultracentrifugation spin at 45,000 RPM in a TLA100.1 rotor for 30 minutes  
416 at 4°C. The lipid droplet layer at the top of the centrifugation tube was aspirated, and  
417 contaminating organelles were removed by an additional centrifugation of the lipid droplet fraction.  
418 The final volume of lipid droplet and cytosol fractions were kept consistent across conditions.

419

#### 420 **Immunoblotting**

421 Protein lysates were collected from worms using RIPA buffer (50 mM Tris-HCl, 250 mM sucrose,  
422 1 mM EDTA, and Roche protease inhibitor tablet, with 1% or 5% SDS) and a handheld  
423 homogenizer, and cleared lysate protein concentrations were quantified using the DC Protein  
424 Assay kit (BIO-RAD). Equal amounts of total protein (10 µg) or comparative volumes for lipid  
425 droplet fractions (Input volume is 10% of lipid droplet and cytosol fractions) were separated by  
426 SDS-PAGE on a 4-15% Tris-Glycine gel and transferred to nitrocellulose. The membrane was  
427 briefly stained with Ponceau S to confirm even transfer, rinsed with TBS-T until clear, blocked  
428 with 5% nonfat dry milk in TBS-T, and immunoblotted with anti-Ubiquitin (Invitrogen MAI-10035),  
429 anti-GFP (Santa Cruz SC-8334), and anti-Actin (Millipore, MAB1501R). The membrane was  
430 developed using SuperSignal West Femto Maximum Sensitivity Substrate (ThermoFisher) and  
431 imaged on a ChemiDoc Imaging System (BIO-RAD).

432

#### 433 **CONTRIBUTIONS**

434 AVK, JM, WP and JAL performed lifespan analyses and imaging as well as RNAi sequencing,  
435 validation, and analysis. AVK, JM, JAL and JRJ validated the whole-genome RNAi screening. JM

436 performed the RNA sequencing and lipid droplet analyses. WP conducted lipid staining and AVK  
437 performed the confocal microscopy imaging. CN, RP and JLA performed lifespan analysis  
438 repeats. SQW and WP developed SQST-1 over-expressing and tandem reporter strains. LRL  
439 designed the experiments, conducted initial RNAi screening, imaging and lifespan analyses, and  
440 wrote the manuscript. All co-authors edited the manuscript.

441

## 442 **ACKNOWLEDGEMENTS**

443 We are grateful for the technical support provided by Erin McConnell, Diego Rodriguez, Rachel  
444 Tam and Tuong Tran. We thank the Malene Hansen laboratory (SBPMDI) and the Caenorhabditis  
445 Genetics Center (U. Minnesota, P40 OD010440) for providing transgenic and mutant strains and  
446 the Andrew Dillin laboratory (UC Berkeley/HHMI) for sharing expression plasmids. This work was  
447 funded by grants from the National Institute of Health (R00 AG042494, R01 AG051810 and R21  
448 AG068922) and a Glenn Award for Research in Biological Mechanisms of Aging from the Glenn  
449 Foundation for Medical Research to LRL.

450

## 451 **REFERENCES**

- 452 1 Koga, H., Kaushik, S. & Cuervo, A. M. Protein homeostasis and aging: The importance of  
453 exquisite quality control. *Ageing Res Rev* **10**, 205-215 (2011).
- 454 2 Reis-Rodrigues, P. *et al.* Proteomic analysis of age-dependent changes in protein  
455 solubility identifies genes that modulate lifespan. *Aging Cell* **11**, 120-127 (2012).
- 456 3 Sui, X. *et al.* Widespread remodeling of proteome solubility in response to different protein  
457 homeostasis stresses. *Proc Natl Acad Sci U S A* **117**, 2422-2431 (2020).
- 458 4 Walther, D. M. *et al.* Widespread Proteome Remodeling and Aggregation in Aging *C.*  
459 *elegans*. *Cell* **161**, 919-932 (2015).

460 5 Ben-Zvi, A., Miller, E. A. & Morimoto, R. I. Collapse of proteostasis represents an early  
461 molecular event in *Caenorhabditis elegans* aging. *Proc Natl Acad Sci U S A* **106**, 14914-  
462 14919 (2009).

463 6 Vilchez, D. *et al.* RPN-6 determines *C. elegans* longevity under proteotoxic stress  
464 conditions. *Nature* **489**, 263-268 (2012).

465 7 Chang, J. T., Kumsta, C., Hellman, A. B., Adams, L. M. & Hansen, M. Spatiotemporal  
466 regulation of autophagy during *Caenorhabditis elegans* aging. *eLife* **6** (2017).

467 8 Lapierre, L. R. *et al.* The TFEB orthologue HLH-30 regulates autophagy and modulates  
468 longevity in *Caenorhabditis elegans*. *Nat Commun* **4**, 2267 (2013).

469 9 Morley, J. F. & Morimoto, R. I. Regulation of longevity in *Caenorhabditis elegans* by heat  
470 shock factor and molecular chaperones. *Mol Biol Cell* **15**, 657-664 (2004).

471 10 Tikku, V. *et al.* Small nucleoli are a cellular hallmark of longevity. *Nat Commun* **8**, 16083  
472 (2017).

473 11 Visscher, M. *et al.* Proteome-wide Changes in Protein Turnover Rates in *C. elegans*  
474 Models of Longevity and Age-Related Disease. *Cell Rep* **16**, 3041-3051 (2016).

475 12 Dhondt, I. *et al.* FOXO/DAF-16 Activation Slows Down Turnover of the Majority of Proteins  
476 in *C. elegans*. *Cell Rep* **16**, 3028-3040 (2016).

477 13 Kirkin, V. & Rogov, V. V. A Diversity of Selective Autophagy Receptors Determines the  
478 Specificity of the Autophagy Pathway. *Mol Cell* **76**, 268-285 (2019).

479 14 Pankiv, S. *et al.* p62/SQSTM1 binds directly to Atg8/LC3 to facilitate degradation of  
480 ubiquitinated protein aggregates by autophagy. *J Biol Chem* **282**, 24131-24145 (2007).

481 15 Aparicio, R., Hansen, M., Walker, D. W. & Kumsta, C. The selective autophagy receptor  
482 SQSTM1/p62 improves lifespan and proteostasis in an evolutionarily conserved manner.  
483 *Autophagy* **16**, 772-774 (2020).

484 16 Kumsta, C. *et al.* The autophagy receptor p62/SQST-1 promotes proteostasis and  
485 longevity in *C. elegans* by inducing autophagy. *Nat Commun* **10**, 5648 (2019).

486 17 Aparicio, R., Rana, A. & Walker, D. W. Upregulation of the Autophagy Adaptor  
487 p62/SQSTM1 Prolongs Health and Lifespan in Middle-Aged Drosophila. *Cell Rep* **28**,  
488 1029-1040 e1025 (2019).

489 18 Palikaras, K., Lionaki, E. & Tavernarakis, N. Coordination of mitophagy and mitochondrial  
490 biogenesis during ageing in *C. elegans*. *Nature* **521**, 525-528 (2015).

491 19 Johansen, T. & Lamark, T. Selective autophagy mediated by autophagic adapter proteins.  
492 *Autophagy* **7**, 279-296 (2011).

493 20 Zhang, B. *et al.* Brain-gut communications via distinct neuroendocrine signals  
494 bidirectionally regulate longevity in *C. elegans*. *Genes Dev* **32**, 258-270 (2018).

495 21 Antebi, A. Regulation of longevity by the reproductive system. *Exp Gerontol* **48**, 596-602  
496 (2013).

497 22 Gelino, S. *et al.* Intestinal Autophagy Improves Healthspan and Longevity in *C. elegans*  
498 during Dietary Restriction. *PLoS Genet* **12**, e1006135 (2016).

499 23 Lapierre, L. R., Gelino, S., Melendez, A. & Hansen, M. Autophagy and lipid metabolism  
500 coordinately modulate life span in germline-less *C. elegans*. *Curr Biol* **21**, 1507-1514  
501 (2011).

502 24 Wang, M. C., O'Rourke, E. J. & Ruvkun, G. Fat metabolism links germline stem cells and  
503 longevity in *C. elegans*. *Science* **322**, 957-960 (2008).

504 25 Lapierre, L. R., Melendez, A. & Hansen, M. Autophagy links lipid metabolism to longevity  
505 in *C. elegans*. *Autophagy* **8**, 144-146 (2012).

506 26 Chapin, H. C., Okada, M., Merz, A. J. & Miller, D. L. Tissue-specific autophagy responses  
507 to aging and stress in *C. elegans*. *Aging (Albany NY)* **7**, 419-434 (2015).

508 27 Ramachandran, P. V. *et al.* Lysosomal Signaling Promotes Longevity by Adjusting  
509 Mitochondrial Activity. *Dev Cell* **48**, 685-696 e685 (2019).

510 28 Folick, A. *et al.* Aging. Lysosomal signaling molecules regulate longevity in *Caenorhabditis*  
511 *elegans*. *Science* **347**, 83-86 (2015).

512 29 Seah, N. E. *et al.* Autophagy-mediated longevity is modulated by lipoprotein biogenesis.  
513 *Autophagy* **12**, 261-272 (2016).

514 30 O'Rourke, E. J., Soukas, A. A., Carr, C. E. & Ruvkun, G. C. *elegans* major fats are stored  
515 in vesicles distinct from lysosome-related organelles. *Cell Metab* **10**, 430-435 (2009).

516 31 Lapierre, L. R. *et al.* Autophagy genes are required for normal lipid levels in *C. elegans*.  
517 *Autophagy* **9**, 278-286 (2013).

518 32 Brooks, K. K., Liang, B. & Watts, J. L. The influence of bacterial diet on fat storage in *C.*  
519 *elegans*. *PLoS One* **4**, e7545 (2009).

520 33 Perez, C. L. & Van Gilst, M. R. A <sup>13</sup>C isotope labeling strategy reveals the influence of  
521 insulin signaling on lipogenesis in *C. elegans*. *Cell Metab* **8**, 266-274 (2008).

522 34 Kirkwood, T. B. & Holliday, R. The evolution of ageing and longevity. *Proc R Soc Lond B*  
523 *Biol Sci* **205**, 531-546 (1979).

524 35 Narbonne, P. & Roy, R. *Caenorhabditis elegans* dauers need LKB1/AMPK to ration lipid  
525 reserves and ensure long-term survival. *Nature* **457**, 210-214 (2009).

526 36 Miller, H. *et al.* Genetic interaction with temperature is an important determinant of  
527 nematode longevity. *Aging Cell* **16**, 1425-1429 (2017).

528 37 Lapierre, L. R., Kumsta, C., Sandri, M., Ballabio, A. & Hansen, M. Transcriptional and  
529 epigenetic regulation of autophagy in aging. *Autophagy* **11**, 867-880 (2015).

530 38 Kelmer Sacramento, E. *et al.* Reduced proteasome activity in the aging brain results in  
531 ribosome stoichiometry loss and aggregation. *Mol Syst Biol* **16**, e9596 (2020).

532 39 Zhang, P. *et al.* Proteomic study and marker protein identification of *Caenorhabditis*  
533 *elegans* lipid droplets. *Mol Cell Proteomics* **11**, 317-328 (2012).

534 40 Vrablik, T. L., Petyuk, V. A., Larson, E. M., Smith, R. D. & Watts, J. L. Lipidomic and  
535 proteomic analysis of *Caenorhabditis elegans* lipid droplets and identification of ACS-4 as  
536 a lipid droplet-associated protein. *Biochim Biophys Acta* **1851**, 1337-1345 (2015).

537 41 Zechner, R., Kienesberger, P. C., Haemmerle, G., Zimmermann, R. & Lass, A. Adipose  
538 triglyceride lipase and the lipolytic catabolism of cellular fat stores. *J Lipid Res* **50**, 3-21  
539 (2009).

540 42 Olzmann, J. A. & Carvalho, P. Dynamics and functions of lipid droplets. *Nat Rev Mol Cell*  
541 *Biol* **20**, 137-155 (2019).

542 43 Denzel, M. S., Lapierre, L. R. & Mack, H. I. D. Emerging topics in *C. elegans* aging  
543 research: Transcriptional regulation, stress response and epigenetics. *Mech Ageing Dev*  
544 **177**, 4-21 (2019).

545 44 Moldavski, O. *et al.* Lipid Droplets Are Essential for Efficient Clearance of Cytosolic  
546 Inclusion Bodies. *Dev Cell* **33**, 603-610 (2015).

547 45 Mejhert, N. *et al.* Partitioning of MLX-Family Transcription Factors to Lipid Droplets  
548 Regulates Metabolic Gene Expression. *Mol Cell* **77**, 1251-1264 e1259 (2020).

549 46 Zhang, S. O. *et al.* Genetic and dietary regulation of lipid droplet expansion in  
550 *Caenorhabditis elegans*. *Proc Natl Acad Sci U S A* **107**, 4640-4645 (2010).

551 47 Zaarur, N. *et al.* ATGL-1 mediates the effect of dietary restriction and the insulin/IGF-1  
552 signaling pathway on longevity in *C. elegans*. *Mol Metab* **27**, 75-82 (2019).

553 48 Olzmann, J. A., Richter, C. M. & Kopito, R. R. Spatial regulation of UBXD8 and p97/VCP  
554 controls ATGL-mediated lipid droplet turnover. *Proc Natl Acad Sci U S A* **110**, 1345-1350  
555 (2013).

556 49 Wu, X. & Rapoport, T. A. Mechanistic insights into ER-associated protein degradation.  
557 *Curr Opin Cell Biol* **53**, 22-28 (2018).

558 50 Bug, M. & Meyer, H. Expanding into new markets--VCP/p97 in endocytosis and  
559 autophagy. *J Struct Biol* **179**, 78-82 (2012).

560 51 Hill, S. M. *et al.* VCP/p97 regulates Beclin-1-dependent autophagy initiation. *Nat Chem*  
561 *Biol* **17**, 448-455 (2021).

562 52 Vembar, S. S. & Brodsky, J. L. One step at a time: endoplasmic reticulum-associated  
563 degradation. *Nat Rev Mol Cell Biol* **9**, 944-957 (2008).

564 53 Demishtein, A. *et al.* SQSTM1/p62-mediated autophagy compensates for loss of  
565 proteasome polyubiquitin recruiting capacity. *Autophagy* **13**, 1697-1708 (2017).

566 54 Korolchuk, V. I., Mansilla, A., Menzies, F. M. & Rubinsztein, D. C. Autophagy inhibition  
567 compromises degradation of ubiquitin-proteasome pathway substrates. *Mol Cell* **33**, 517-  
568 527 (2009).

569 55 McColl, G. *et al.* Utility of an improved model of amyloid-beta (A $\beta$ (1-42)) toxicity in  
570 *Caenorhabditis elegans* for drug screening for Alzheimer's disease. *Mol Neurodegener* **7**,  
571 57 (2012).

572 56 Franz, A., Ackermann, L. & Hoppe, T. Create and preserve: proteostasis in development  
573 and aging is governed by Cdc48/p97/VCP. *Biochim Biophys Acta* **1843**, 205-215 (2014).

574 57 Roberts, M. A. & Olzmann, J. A. Protein Quality Control and Lipid Droplet Metabolism.  
575 *Annu Rev Cell Dev Biol* **36**, 115-139 (2020).

576 58 Bersuker, K. & Olzmann, J. A. Establishing the lipid droplet proteome: Mechanisms of lipid  
577 droplet protein targeting and degradation. *Biochim Biophys Acta Mol Cell Biol Lipids* **1862**,  
578 1166-1177 (2017).

579 59 Galluzzi, L., Bravo-San Pedro, J. M., Levine, B., Green, D. R. & Kroemer, G.  
580 Pharmacological modulation of autophagy: therapeutic potential and persisting obstacles.  
581 *Nat Rev Drug Discov* **16**, 487-511 (2017).

582 60 Zaffagnini, G. *et al.* Phasing out the bad-How SQSTM1/p62 sequesters ubiquitinated  
583 proteins for degradation by autophagy. *Autophagy* **14**, 1280-1282 (2018).

584 61 Baskoylu, S. N. Disrupted Autophagy and Neuronal Dysfunction in *C. elegans* Knock-in  
585 Models of FUS Amyotrophic Lateral Sclerosis. *BioRxiv* 799932 (2020).

586 62 Zaffagnini, G. *et al.* p62 filaments capture and present ubiquitinated cargos for autophagy.  
587 *EMBO J* **37** (2018).



588 63 Hansen, M., Flatt, T. & Aguilaniu, H. Reproduction, fat metabolism, and life span: what is  
589 the connection? *Cell Metab* **17**, 10-19 (2013).

590 64 Silvestrini, M. J. *et al.* Nuclear Export Inhibition Enhances HLH-30/TFEB Activity,  
591 Autophagy, and Lifespan. *Cell Rep* **23**, 1915-1921 (2018).

592 65 Schmitz, G. & Grandl, M. Lipid homeostasis in macrophages - implications for  
593 atherosclerosis. *Rev Physiol Biochem Pharmacol* **160**, 93-125 (2008).

594 66 Marschallinger, J. *et al.* Lipid-droplet-accumulating microglia represent a dysfunctional  
595 and proinflammatory state in the aging brain. *Nat Neurosci* **23**, 194-208 (2020).

596 67 Nguyen, T. B. *et al.* DGAT1-Dependent Lipid Droplet Biogenesis Protects Mitochondrial  
597 Function during Starvation-Induced Autophagy. *Dev Cell* **42**, 9-21 e25 (2017).

598 68 Di Paolo, G. & Kim, T. W. Linking lipids to Alzheimer's disease: cholesterol and beyond.  
599 *Nat Rev Neurosci* **12**, 284-296 (2011).

600 69 Inloes, J. M. *et al.* The hereditary spastic paraplegia-related enzyme DDHD2 is a principal  
601 brain triglyceride lipase. *Proc Natl Acad Sci U S A* **111**, 14924-14929 (2014).

602 70 Yang, L. *et al.* Neuronal lipolysis participates in PUFA-mediated neural function and  
603 neurodegeneration. *EMBO Rep* **21**, e50214 (2020).

604 71 Nuriel, T. *et al.* Neuronal hyperactivity due to loss of inhibitory tone in APOE4 mice lacking  
605 Alzheimer's disease-like pathology. *Nat Commun* **8**, 1464 (2017).

606 72 Labbadia, J. & Morimoto, R. I. The biology of proteostasis in aging and disease. *Annu Rev*  
607 *Biochem* **84**, 435-464 (2015).

608 73 Brenner, S. The genetics of *Caenorhabditis elegans*. *Genetics* **77**, 71-94 (1974).

609 74 Stiernagle, T. Maintenance of *C. elegans*. *WormBook*, 1-11 (2006).

610 75 Kamath, R. S. *et al.* Systematic functional analysis of the *Caenorhabditis elegans* genome  
611 using RNAi. *Nature* **421**, 231-237 (2003).

612 76 Hansen, M., Hsu, A. L., Dillin, A. & Kenyon, C. New genes tied to endocrine, metabolic,  
613 and dietary regulation of lifespan from a *Caenorhabditis elegans* genomic RNAi screen.  
614 *PLoS Genet* **1**, 119-128 (2005).

615 77 Holdorf, A. D. *et al.* WormCat: An Online Tool for Annotation and Visualization of  
616 *Caenorhabditis elegans* Genome-Scale Data. *Genetics* **214**, 279-294 (2020).

617

# Figures

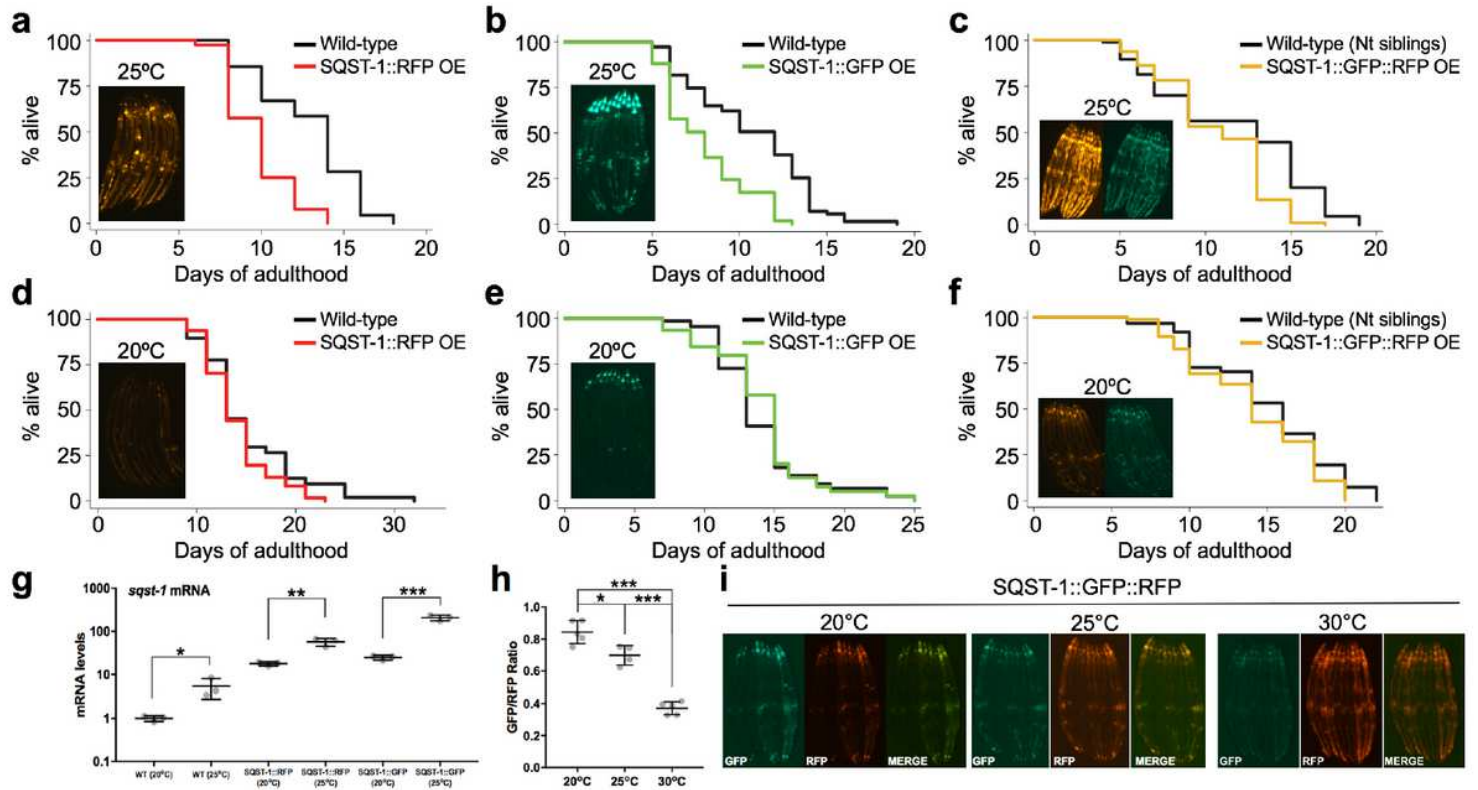


**Figure 1**

SQST-1 dynamics and lifespan modulation is temperature-dependent in *C. elegans* a-f. Lifespan analysis of wild-type animals and animals over-expressing SQST-1 fused to RFP, GFP or GFP::RFP fed OP50 *E. coli*, developmentally raised at 20°C and then grown at 25°C (a-c) or 20°C (d-f) during adulthood (n=100). Insets include mRNA corresponding representative images of transgenic animals at Day 5 of adulthood. g. *sqst-1* mRNA levels in wild-type and transgenic animals were quantified by qPCR. Biological triplicates  $\pm$ SD t-test \*p<0.05, \*\*p<0.01, \*\*\*p<0.001 h. Levels of GFP and RFP were measured in transgenic tandem SQST-1::GFP::RFP animals after incubating Day 1 animals at 20°C, 25°C or 30°C for 24 hours. Average of 10 worms per image. n=5 images per condition  $\pm$ SD ANOVA \*p<0.05, \*\*p<0.01, \*\*\*p<0.001 i. Representative images of transgenic animals (quantified in h.) incubated at 20°C, 25°C or 30°C for 24 hours. Details about lifespan analyses and repeats are available in Supplemental Table 4.

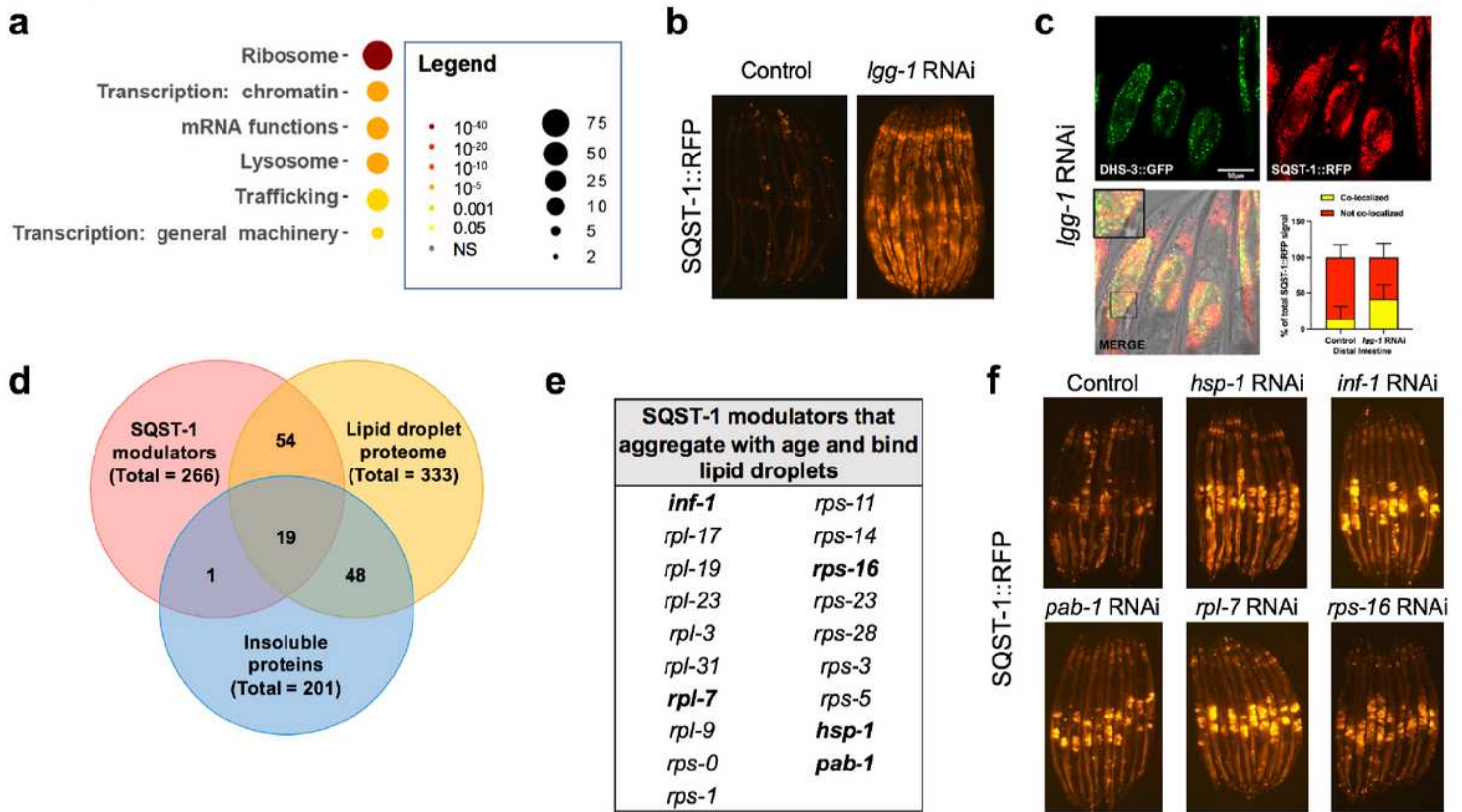


**Figure 2**

SQST-1 regulators include proteins that bind lipid droplets and that aggregate with age a. Pathway enrichment of genes that regulate SQST-1 levels using WormCat77. b. SQST-1::RFP accumulates after autophagy is inhibited by *lgg-1* silencing for 3 days during adulthood. c. Representative confocal microscopy image of the distal intestine of animals expressing both SQST-1::RFP and the lipid droplet-resident protein DHS-3 fused to GFP, subjected to *lgg-1* silencing for 3 days during adulthood. The localization between DHS-3::GFP and SQST-1::GFP is quantified in control bacteria-treated animals and animals fed bacteria expressing dsRNA against *lgg-1* for 3 days ( $\pm$ SD). d. Overlap of SQST-1 regulators with age-dependent aggregating proteins<sup>2</sup> and lipid droplet-associated proteins<sup>40</sup>. e. Identity of 19 overlapping genes from d. f. Representative images of gene silencing of a set of overlapping SQST-1 regulators during adulthood (3 days) in animals over-expressing SQST-1::RFP. Details about SQST-1 regulators are available in Supplemental Tables 1 and 2.

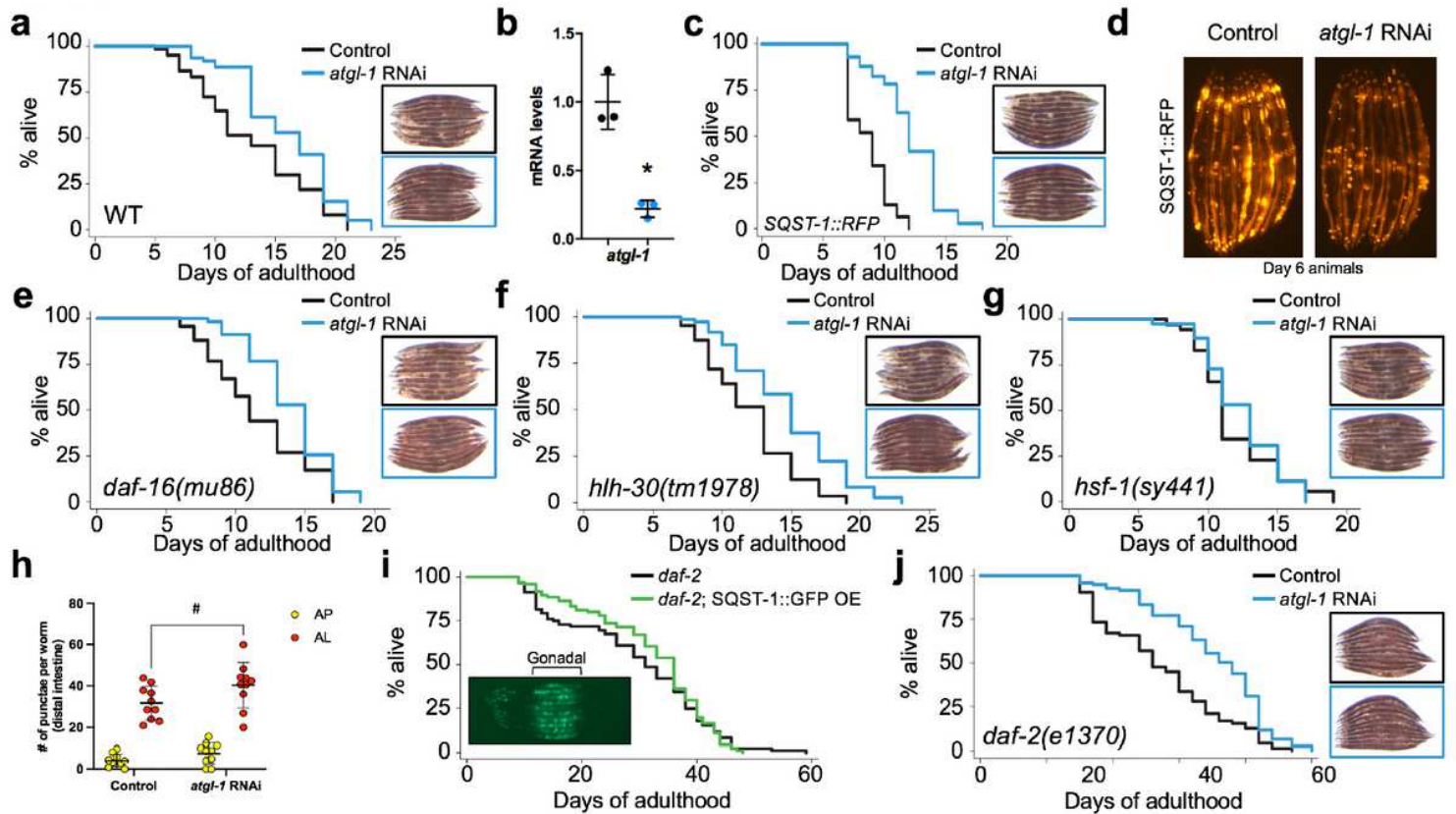


**Figure 3**

Silencing *atgl-1* extends lifespan and reduces SQST-1 accumulation in *C. elegans*. a. Lifespan analysis of wild-type WT animals and c. animals over-expressing SQST-1::RFP raised at 20°C on OP50 *E. coli* and then grown at 25°C during adulthood on control bacteria or bacteria expressing dsRNA against *atgl-1* (n=100). Corresponding images of Day 5 animals stained with Oil-Red-O demonstrating intestinal lipid store accretion under *atgl-1* RNAi (blue borders). b. Levels of *atgl-1* mRNA measured by qPCR showing efficient silencing after 3 days on *atgl-1* RNAi (Black: Control RNAi, Blue: *atgl-1* RNAi). Biological triplicates t-test \*p<0.05 d. Representative fluorescence images taken after Day 1 animals over-expressing SQST-1::RFP and DHS-3::GFP were fed control bacteria or bacteria expressing dsRNA against *atgl-1* for 5 days at 25°C. e-g. Lifespan analysis of *daf-16(mu86)*, *hlh-30(tm1978)*, and *hsf-1(sy441)* mutants raised at 20°C on OP50 *E. coli* and then grown at 25°C during adulthood on control bacteria or bacteria expressing dsRNA against *atgl-1* (n=100). Corresponding images of Day 5 animals stained with ORO demonstrating intestinal lipid store accretion under *atgl-1* RNAi (blue borders). h. Levels of autophagosomes and autolysosomes were measured in animals expressing the tandem reporter mCherry::GFP::LGG-17 after feeding Day 1 animals with control bacteria or bacteria expressing dsRNA against *atgl-1* for 2 days at 25°C. n=10 per condition ±SD t-test #p<0.06 i. Lifespan analysis of *daf-2(e1370)* and *daf-2;SQST-1::GFP* animals raised at 20°C and then grown at 25°C during adulthood on OP50 *E. coli* (with representative image of Day 5 animals, comparative image of wild-type animals in Figure 1b). j. *daf-2(e1370)* animals were raised at 20°C on OP50 *E. coli* and then grown at 25°C during adulthood on control bacteria or bacteria expressing dsRNA against *atgl-1* (n=100). Corresponding images of Day 5 animals stained with

ORO demonstrating intestinal lipid store accretion under *atgl-1* RNAi (blue borders). Details about lifespan analyses and repeats are available in Supplemental Tables 3 and 4.

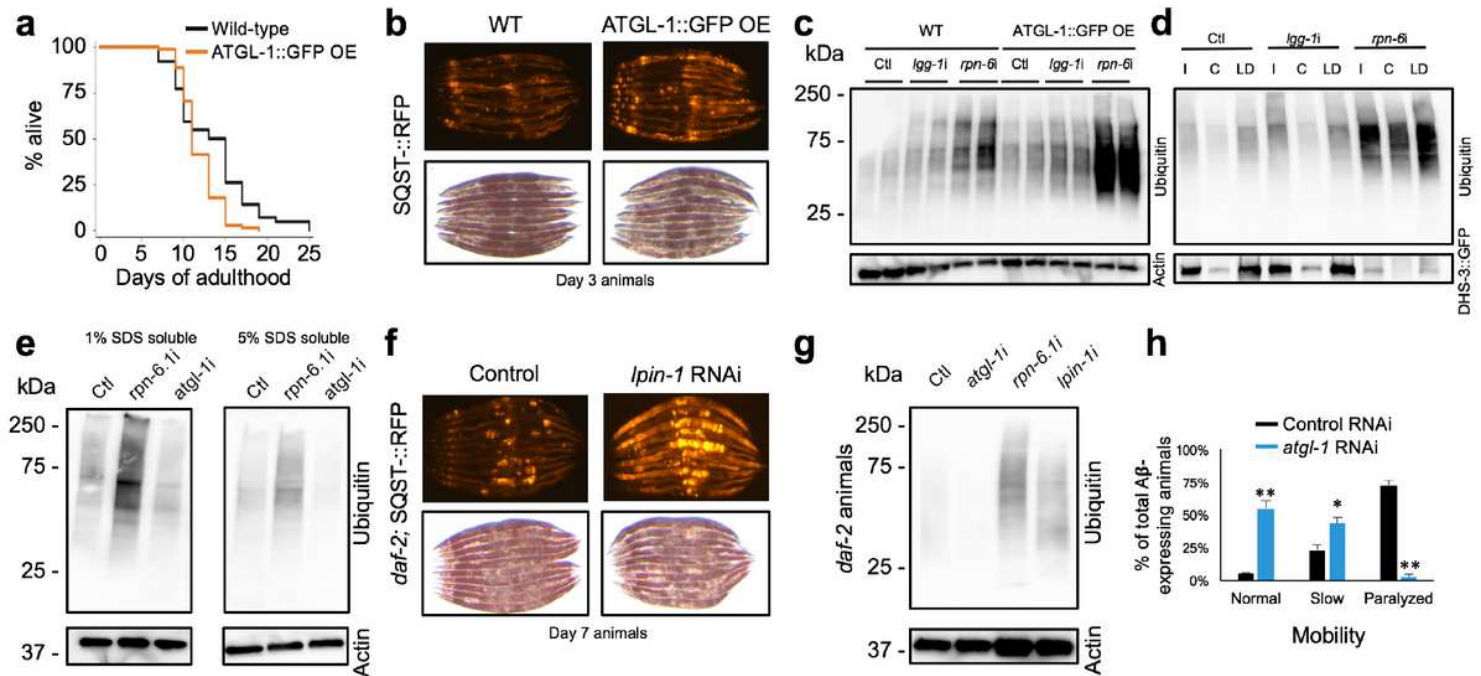


**Figure 4**

Lipid droplets modulate protein ubiquitination levels and enhance proteostasis a. Lifespan analysis of wild-type and transgenic animals over-expressing ATGL-1::GFP developmentally raised at 20°C and then grown at 25°C during adulthood on OP50 *E. coli* (n=100). b. Levels of RFP signal and lipid droplets from Day 3 animals over-expressing SQST-1::RFP in wild-type or transgenic ATGL-1::GFP over-expressing background. c. Wild-type and ATGL-1::GFP over-expressing animals were raised at 20°C and then grown at 25°C during adulthood on control bacteria (Ctl) or bacteria expressing dsRNA against autophagy gene *lgg-1* or proteasome subunit gene *rpn-6.1* for 2 days. Levels of ubiquitinated proteins and actin were visualized by immunoblotting. Biological replicates shown. d. Animals expressing lipid droplet-resident protein DHS-3 fused to GFP were raised at 20°C and then grown at 25°C during adulthood on control bacteria or bacteria expressing RNAi against *lgg-1* or *rpn-6* for 4 days. Levels of ubiquitinated proteins and DHS-3::GFP were visualized by immunoblotting from total input (I), cytosol (C) and lipid droplet (LD) fractions (comparative% loaded between fractions, i.e. 10%). e. Day 1 wild-type animals were fed control bacteria or bacteria expressing dsRNA against *rpn-6* or *atgl-1* for 3 days and ubiquitination levels were detected by immunoblotting. f. Levels of RFP signal and lipid droplets in Day 7 *daf-2* animals over-expressing SQST-1::RFP and fed control bacteria or bacteria expressing dsRNA against *lpin-1* during adulthood. g. Day 1 *daf-2* animals were fed control bacteria or bacteria expressing dsRNA against *atgl-1*, *rpn-6* or *lpin-1* for 5 days at 25°C and ubiquitination levels were detected by immunoblotting. h. Nematodes expressing heat-inducible human A $\beta$ -42 were grown at 20°C on OP50 *E. coli* and fed control bacteria or bacteria expressing dsRNA against *atgl-1* at Day 1 of adulthood for 2 days at 25°C. Paralysis was scored thereafter. Triplicates of n=100 each,  $\pm$ SD t-test \*p<0.05, \*\*p<0.01.

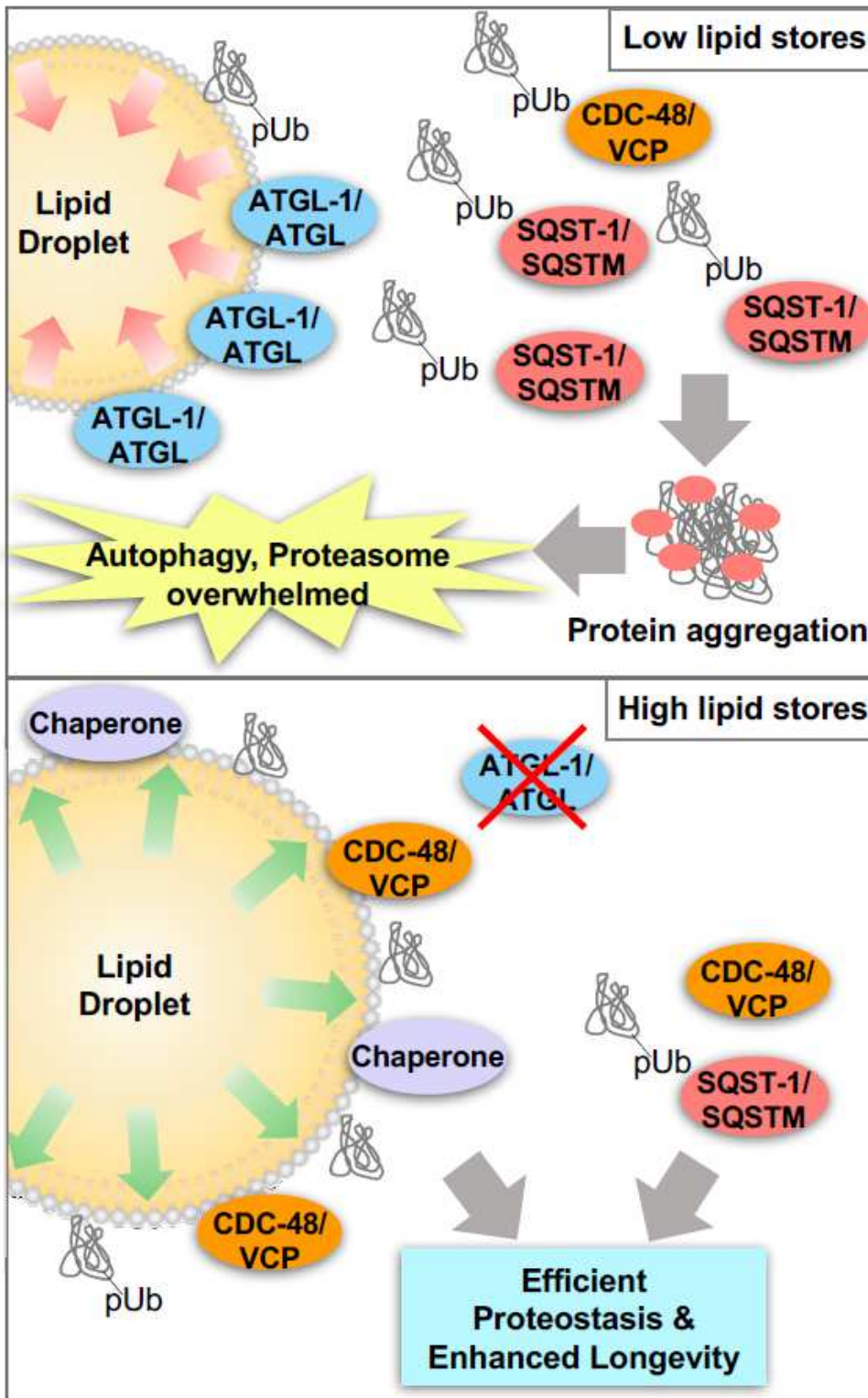


Figure 5

Lipid droplets buffer proteostasis by harboring proteins that challenge protein degradation pathways. When lipid stores are low, ubiquitinated proteins accumulate and eventually overwhelm the proteasomal system and selective autophagy receptors such as SQST-1. High lipid droplet content increases the capacity of cells to stabilize proteins (in conjunction with CDC-48 and HSF-1-regulated chaperones, such as HSP-1) that would otherwise accumulate and aggregate. As proteostasis declines with age, lipid

droplets can facilitate autophagic degradation and stabilize the proteome, which prevents the burdening of selective autophagy.

## Supplementary Files

This is a list of supplementary files associated with this preprint. Click to download.

- [SupplementalTable1FINAL042221.xlsx](#)
- [SupplementalTable2FINAL042221.xlsx](#)
- [P62ManuscriptSuppFigures2021LRFINAL042121.pdf](#)